OL | Organic Letters

Cite This: Org. Lett. XXXX, XXX, XXX−XXX

Letter

pubs.acs.org/OrgLett

Mechanistic Insight into the Catalytic Staudinger Ligation

Paul B. White,*[,†,‡] Sjoerd J. Rijpkema,[†,‡] Roderick P. Bunschoten,[†] and Jasmin Mecinović*[,†,§]

[†]Institute for Molecules and Materials, Radboud University, Heyendaalseweg 135, 6525 AJ Nijmegen, The Netherlands

[§]Department of Physics, Chemistry and Pharmacy, University of Southern Denmark, Campusvej 55, 5230 Odense, Denmark

Supporting Information

ABSTRACT: Organophosphorus-catalyzed Staudinger ligation between carboxylic acids and azides in the presence of phenylsilane reductant produces amides. NMR-based mechanistic investigations revealed that the catalytic Staudinger ligation does not proceed via reduction of phosphine oxide but rather via reduction of iminophosphorane, which can subsequently undergo several transformations to produce the amide product.

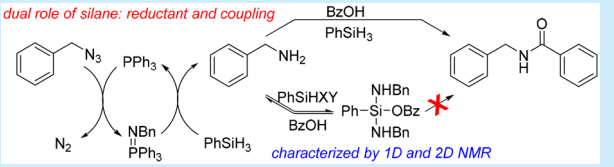

Organophosphorus-mediated reactions have found a widespread use in synthetic organic chemistry.[1] Well-established examples include the Wittig reaction, Mitsunobu reaction, Appel reaction, Staudinger reduction, and Staudinger ligation, which have enabled the transformations of many common functional groups and greatly contributed to the construction of complex molecules of biomedical importance.[1] Recent efforts have demonstrated the development of catalytic versions of these classic reactions along with related reactions.[2] Organophosphorus catalysis typically requires the presence of silane-based reducing agents involved in the chemoselective reduction of phosphine oxides to phosphines during the catalytic cycle.[3]

The Staudinger ligation has been of paramount importance for examinations of various molecular and biomolecular systems.[4] The first catalytic Staudinger ligation was described by Ashfeld et al. in 2012.[2f] The reported Ph_3P-catalyzed Staudinger ligation between carboxylic acids and azides in the presence of phenylsilane led to the formation of a diverse set of amides in very good yields.[2f] Limited mechanistic work suggested that the catalytic reaction importantly relies on the efficient $PhSiH_3$-mediated reduction of Ph_3PO to Ph_3P, which then enters a new catalytic cycle. Recently, Denton et al. challenged this proposed mechanism by suggesting that the organophosphorus-catalyzed reaction proceeds via an alternative pathway through in situ formation of silyl esters.[5] Herein, we report advanced NMR spectroscopic studies on the organophosphorus-catalyzed Staudinger ligation that enables the elucidation of the most plausible mechanism. Our mechanistic studies suggest that (1) Ph_3PO reduction is kinetically unfeasible for being on-cycle and (2) reduction of the iminophosphorane results in either unreactive silylamine species or benzylamine, which reacts with benzoic acid to form amide.

We initially carried out the time-course of the catalytic Staudinger ligation and examined the formation of intermediates and products by ^1H and ^{31}P NMR spectroscopy (Figure 1 and Figures S1 and S2). Heating of benzoic acid **1** (1.0 equiv) and benzyl azide **2** (1.2 equiv) in the presence of

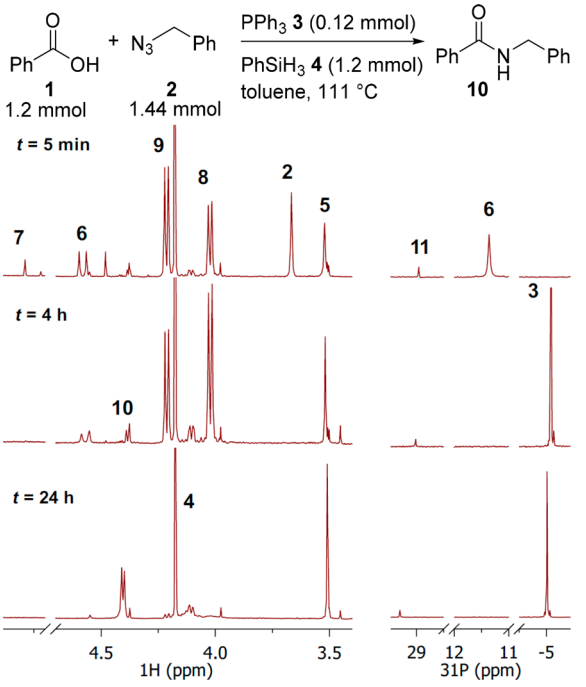

Figure 1. Time-course of the catalytic Staudinger ligation.

Ph_3P **3** (0.1 equiv) and $PhSiH_3$ **4** (1.0 equiv) in anhydrous toluene at 111 °C under argon led to an immediate (within 5 min) formation of benzylamine **5**, iminophosphorane **6**, silyl ester **7**, and two benzylamine-containing species **8** (minor) and **9** (major). Within 4 h, the starting azide **2** was fully consumed, and the formation of the *N*-benzylbenzamide product **10** was clearly observed. Both benzylamine-containing species were still found after 4 h; the ratio, however, was reversed in favor of **8**. A prolonged incubation (24 h) resulted in the disappearance

Received: December 18, 2018

DOI: 10.1021/acs.orglett.8b04035
Org. Lett. XXXX, XXX, XXX−XXX

of signals that belong to **8**, **9**, and **6** and in a substantial increase in the formation of amide product **10**.

$^{31}P\{^{1}H\}$ NMR spectra supported these findings and revealed that Ph_3PO **11** was not produced during the reaction (the Ph_3PO signal in $^{31}P\{^{1}H\}$ NMR spectrum derives from small amounts present in the starting Ph_3P **3**) (Figure 1). Additional $^{31}P\{^{1}H\}$ NMR-based experiments demonstrated that $PhSiH_3$ alone does not mediate reduction of Ph_3PO to Ph_3P within limits of detection; the presence of benzoic acid, however, increased the yield of **3** to 13% in 4 h (Figure S3). These results suggest that it is unlikely that an efficient catalytic Staudinger ligation proceeds via reduction of Ph_3PO to Ph_3P. It is more likely that the majority of the amide product is formed via a different pathway, as described below.

The unanswered question of how amide is formed led us to investigate the two unknown compounds, **8** and **9**, that are present in high concentration from the beginning of the reaction. The amount of these species decreased over time with concomitant formation of amide **10**, while the concentration of amine **5** remained constant. Denton and co-workers assigned these species as a silylated benzylamine based on comparison of ^{1}H chemical shift and $^{1}H-^{1}H$ *J*-couplings between the CH_2 and NH of similar species from literature.[5] However, a more rigorous characterization was required in order to unambiguously confirm these structures and understand their role in the catalytic Staudinger ligation.

2D NMR analyses enabled the conclusive determination of both structures: **8** as $PhSi(OBz)(NHBn)_2$ and **9** as $PhSi(OBz)_2(NHBn)$ (Figure 2). The $^{1}H-^{13}C$ HSQCED spectrum showed that both **8** and **9** CH_2s were slightly shielded (^{13}C: 45.33 ppm) from free benzylamine (^{13}C: 46.43 ppm) (Figure 2A). The ^{1}Hs exhibited a doublet splitting pattern distinct from the singlets of benzylamine **5** or benzyl azide **2**. A COSY experiment (Figure 2B) revealed the coupling partner to be a triplet at 1.79 and 2.27 ppm for **8** and **9**, respectively, which

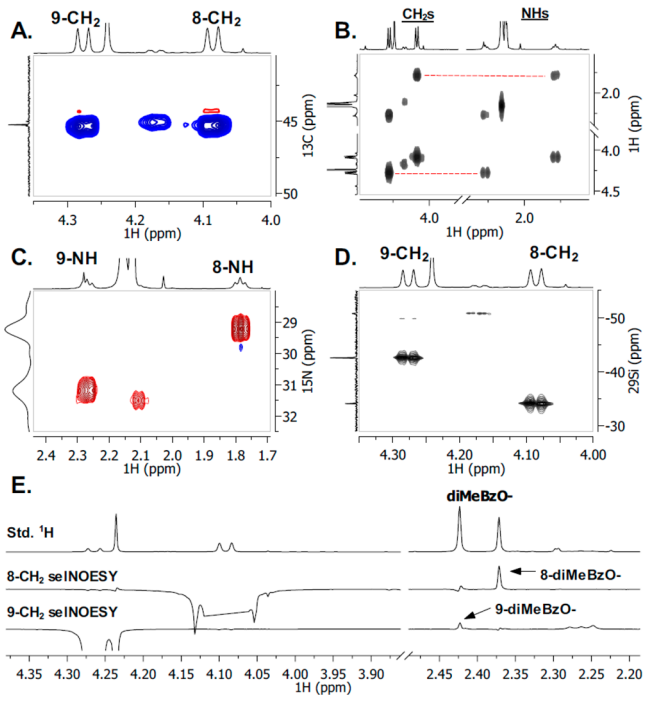

Figure 2. NMR spectroscopic characterization of intermediates **8** and **9**.

were determined to be NHs ($^{1}H-^{15}N$ HSQCED) (Figure 2C). A subsequent $^{1}H-^{29}Si$ HMBC revealed that the CH_2 and NH were connected to a ^{29}Si nucleus at −34.12 ppm (**8**) and −42.58 ppm (**9**) as well as the expected corresponding phenyl groups (Figure 2D). Furthermore, the absence of any ^{1}H cross peaks at those ^{29}Si shifts in the $^{1}H-^{29}Si$ HSQCED spectrum revealed that **8** and **9** must be a quaternary silicon species (Figure 2D). A third minor species was also observed in the ^{1}H spectrum at 4.17 ppm (Figure 2). Similar to **8** and **9**, it was a silylbenzylamine (δ_C = 45.00 ppm; δ_N = 31.44 ppm; δ_{Si} = −50.76 ppm) with an NH group; however, its low abundance made the above analyses more challenging. Diffusion NMR measurements estimated that the unknown intermediate was ∼1.72× heavier than **8** or **9** and thus is likely a bridging species (Figure S4).

Partial structure fragments of the formula $PhSi(Y)_{3-x}(NHBn)_x$ were drawn, and we hypothesized that Y could be OBz or OH. Unfortunately, through-bond measurements between the NH ^{1}H and C═O would be challenging due to the number of bonds in between and through-space measurements were difficult due to the overlap of BzO− with free acid, toluene, Ph_3PO, and $PhSiH_3$. Therefore, 2,6-dimethylbenzoic acid was employed to provide a spectral handle via its unique methyl groups (Scheme 1). The reaction

Scheme 1. NOE and ^{1}H NMR Determination of 8′ and 9′

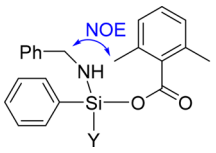

^{1}H NMR Integral Ratios
8′: CH_2:CH_3 = 4:6, Y = NHBn
9′: CH_2:CH_3 = 2:12, Y = 2,6-Me_2OBz

was performed under standard conditions and resulted in nearly identical results as with BzOH. The resulting silylamine doublets were selected for 1D NOESY experiments, which revealed correlations to the acid methyls (Figure 2E). Reciprocal NOEs were observed when selecting the methyl ^{1}Hs. Integrating the singlet of the methyl group and the corresponding doublet of the benzylamine conclusively assigned the formulas $PhSi(OBzMe_2)(NHBn)_2$ (**8′**) and $PhSi(OBzMe_2)_2(NHBn)$ (**9′**) (Figure S5).

These structures are in line with our time-course data (Figure 1); **9** predominantly appears at the early stage of the reaction, when the amount of benzoic acid is high, whereas **8** becomes a dominant species during later stages of the reaction, when an increasing amount of amine is produced. Within 30 min, >95% of the starting benzoic acid could be accounted for as either part of the intermediates **8** and **9** or the product **10**, indicating the rapid reaction and seclusion of free benzoic acid in the reaction mixture.

Since the formation of amide **10** coincided with the decay of **8** and **9**, we were curious as to their formation, dynamics, and reactivity (Figure 1). 1D EXSY (EXchange SpectroscopY) spectra were acquired from catalytic reaction aliquots and measured at 298 K where reactivity is halted (Figure S6). The measurements revealed that the aminobenzyl moieties of **8** and **9** readily exchanged with each other as well as with free benzyl amine (Scheme 2). Additionally, the unknown silylamine species at 4.17 ppm underwent exchange with free benzyl amine and **9**, but not readily with **8**. In the absence of free amine, exchange between **8** and **9** was significantly retarded.

DOI: 10.1021/acs.orglett.8b04035
Org. Lett. XXXX, XXX, XXX−XXX

Scheme 2. Exchange of Intermediates 8 and 9

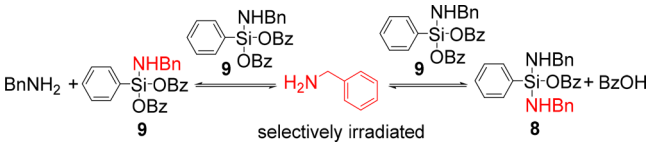

It was unclear whether or not **8** and **9** were off- or on-cycle intermediates in the formation of the amide bond. This could fortunately be probed by slightly altering the reaction conditions. When substoichiometric equivalents of azide (0.25 equiv vs BzOH) were used, the formation of **8** and **9** were avoided altogether. Furthermore, it was revealed that the rate of amide formation was significantly faster; the same quantity of amide (0.1 mmol) was produced in 1 h for the substoichiometric condition compared to 4 h for the standard conditions (Figure 3). This comparative time-course demonstrates that, despite the lower starting azide concentration, faster rates are obtained for amide formation under substoichiometric conditions where **8** and **9** are not present (Figure S7). These results suggest that **8** and **9** are off-cycle intermediates that pool the reactive benzoic acid and benzylamine components. A slow equilibrium is capable of releasing these reagents as they are consumed to form the amide likely via a phenylsilane-mediated process.

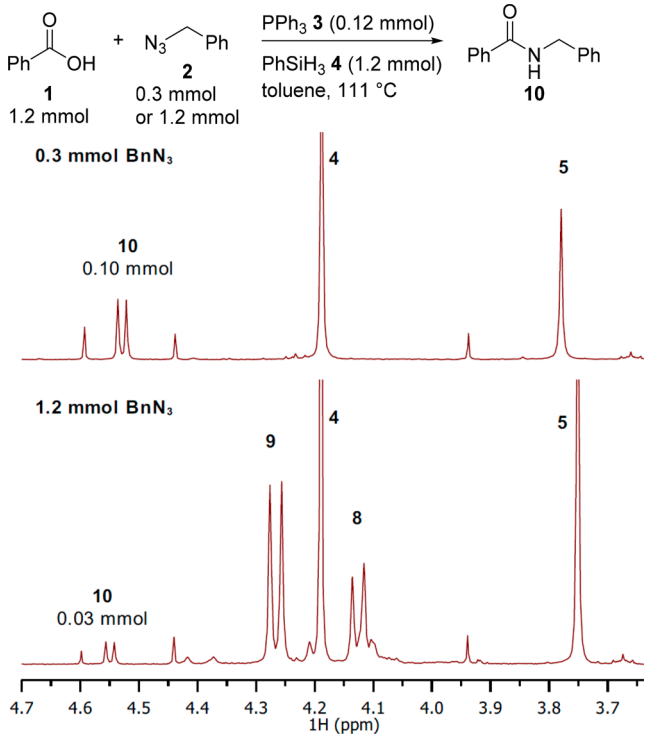

Figure 3. Observation of rate inhibition by **8** and **9** when a substoichiometric quantity (top) or a stoichiometric amount (bottom) of benzyl azide **2** is used. Spectrum represents the reaction at 1 h. Full time course is shown in Figure S7.

To better understand the formation of these silylamine intermediates, we looked at the formation and reactivity of the iminophosphorane **6** due to its role at converting azide into amine-like species. Reaction between phosphine and azide results in quantitative formation of **6** in less than 2 h at room temperature and <30 min at 111 °C. We were interested in observing the reactivity of **6** with different components of the reaction mixture. Addition of phenylsilane to **6** resulted in reduction to the amine **5** and Ph_3P as the sole products (Scheme 3, Figure S8); no silylamine species were observed.

Scheme 3. Reaction of Iminophosphorane 6 with Components of the Catalytic Staudinger Ligation

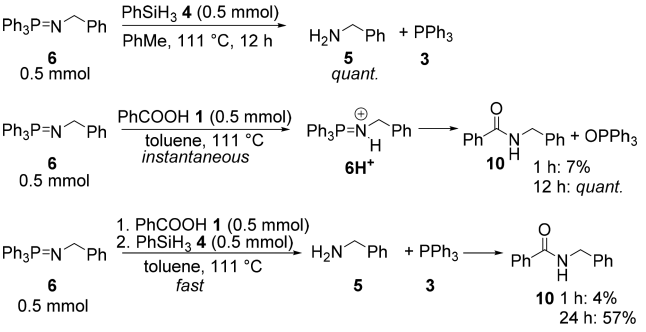

Addition of benzoic acid to **6** resulted in its immediate protonation (**6H**$^+$), as determined by a downfield shift in the $^{31}P\{^1H\}$ spectrum from 5.9 to 36.8 ppm; however, the ^1H shift of the CH_2 did not visibly change (Figure S9). $^{31}P\{^1H\}$ spectra acquired during the catalytic reaction do not reveal **6H**$^+$, implying it is a highly reactive species (Figure 1). Interestingly, without any other additives, **6H**$^+$ spontaneously formed amide **10** and Ph_3PO in refluxing toluene, albeit very slowly (Scheme 3, Figure S9). However, in the presence of $PhSiH_3$, **6H**$^+$ immediately (within 15 min) forms amine and Ph_3P, instead of amide and Ph_3PO, and then progresses to form amide from the reservoir of amine (Scheme 3).

In all cases, species **8** and **9** did not form directly from reaction between **6H**$^+$ and other starting components in the reaction. Therefore, we broadened our investigation to other species present in the reaction mixture at the beginning. Denton et al. identified and synthesized $PhSiH_2OBz$ (**7**) in their mechanistic study, demonstrating its ability to form amide in the presence of azide and phosphine catalyst.[5] Following literature precedent, we synthesized **7** and then introduced different components and intermediates. Excitingly, the reaction between silyl ester **7** and iminophosphorane **6** afforded **8** (55%) and **9** (45%) after 3.5 h at room temperature (Figure S10). Despite the highly reactive nature of silyl ester **7**, when reacted with benzyl amine **5**, it only formed 40% of amide product after 4 days at room temperature (Figure S11).

Free carboxylic acid and amine undergo phenylsilane-mediated amidation in THF at room temperature.[6] In line with this finding, we observed that 58% of amide is formed in toluene at 111 °C after 90 min (Figure S12 and Table S3). In the absence of phenylsilane, the rate was drastically retarded, yielding only 7.3% conversion after 24 h. Addition of catalytic phosphine or phosphine oxide did not impact the rate or results of the stoichiometric silane-mediated coupling; 77−81% yields were observed after 24 h (Table S3).

With these observations in mind, a new catalytic cycle for the Staudinger ligation can be proposed (Scheme 4). Azide **2** first reacts with the phosphine **3** to form the iminophosphorane **6**. Subsequent protonation of **6** is possible by benzoic acid **1**; however, it is not observed in the catalytic reaction as the subsequent reduction by phenylsilane **4** is significantly faster. The reduction of **6H**$^+$ by phenylsilane **4** regenerates Ph_3P **3** and produces amine **5**. The amine **5** can then participate in

DOI: 10.1021/acs.orglett.8b04035
Org. Lett. XXXX, XXX, XXX−XXX

Scheme 4. Proposed Cycle for the Catalytic Staudinger Ligation

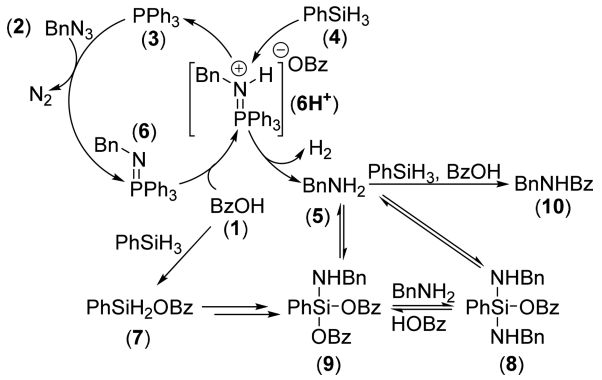

several separate pathways simultaneously. First, it can react with benzoic acid **1** and $PhSiH_3$ **4** to produce amide **10**, as in the stoichiometric reaction. Second, it can act as a base and deprotonate benzoic acid **1**. The benzoic acid **1** can then react with $PhSiH_3$ **4** to form the silyl ester **7**, which is observed at the earliest time points of the reaction. The silyl ester can subsequently react further with **6** to produce a family of off-cycle silylbenzylamine intermediates, **8** and **9**, which sequester the acid and amine. Third, the amine **5** engages in a dynamic equilibrium with **8** and **9** that causes the slow but eventual release of free benzoic acid into solution. The acid and amine then can subsequently react with the remaining phenylsilane to form the amide product.

In summary, our NMR analyses demonstrated that the catalytic Staudinger ligation does not proceed via phosphine oxide but rather via iminophosphorane that upon reaction with phenylsilane can undergo distinct pathways, including via off-cycle silyl species, to produce the amide product. We envision that our mechanistic work will contribute to development of efficient catalytic Staudinger ligation under milder reaction conditions.

■ ASSOCIATED CONTENT

Supporting Information

The Supporting Information is available free of charge on the ACS Publications website at DOI: 10.1021/acs.orglett.8b04035.

NMR analyses (PDF)

■ AUTHOR INFORMATION

Corresponding Authors

*E-mail: p.white@science.ru.nl.
*E-mail: mecinovic@sdu.dk.

ORCID

Jasmin Mecinović: 0000-0002-5559-3822

Author Contributions

‡P.B.W. and S.J.R. contributed equally.

Notes

The authors declare no competing financial interest.

■ REFERENCES

(1) (a) Karanam, P.; Reddy, G. M.; Koppolu, S. R.; Lin, W. *Tetrahedron Lett.* **2018**, *59*, 59. (b) Xu, S.; He, Z. *RSC Adv.* **2013**, *3*, 16885.

(2) (a) Buonomo, J. A.; Aldrich, C. C. *Angew. Chem., Int. Ed.* **2015**, *54*, 13041. (b) Coyle, E. E.; Doonan, B. J.; Holohan, A. J.; Walsh, K. A.; Lavigne, F.; Krenske, E. H.; O'Brien, C. J. *Angew. Chem., Int. Ed.* **2014**, *53*, 12907. (c) Denton, R. M.; An, J.; Adeniran, B. *Chem. Commun.* **2010**, *46*, 3025. (d) Denton, R. M.; An, J.; Adeniran, B.; Blake, A. J.; Lewis, W.; Poulton, A. M. *J. Org. Chem.* **2011**, *76*, 6749. (e) Hamstra, D. F. J.; Lenstra, D. C.; Koenders, T. J.; Rutjes, F. P. J. T.; Mecinović, J. *Org. Biomol. Chem.* **2017**, *15*, 6426. (f) Kosal, A. D.; Wilson, E. E.; Ashfeld, B. L. *Angew. Chem., Int. Ed.* **2012**, *51*, 12036. (g) Lenstra, D. C.; Lenting, P. E.; Mecinović, J. *Green Chem.* **2018**, *20*, 4418. (h) Lenstra, D. C.; Rutjes, F. P. J. T.; Mecinović, J. *Chem. Commun.* **2014**, *50*, 5763. (i) Marsden, S. P.; McGonagle, A. E.; McKeever-Abbas, B. *Org. Lett.* **2008**, *10*, 2589. (j) O'Brien, C. J.; Lavigne, F.; Coyle, E. E.; Holohan, A. J.; Doonan, B. J. *Chem. - Eur. J.* **2013**, *19*, 5854. (k) O'Brien, C. J.; Nixon, Z. S.; Holohan, A. J.; Kunkel, S. R.; Tellez, J. L.; Doonan, B. J.; Coyle, E. E.; Lavigne, F.; Kang, L. J.; Przeworski, K. C. *Chem. - Eur. J.* **2013**, *19*, 15281. (l) O'Brien, C. J.; Tellez, J. L.; Nixon, Z. S.; Kang, L. J.; Carter, A. L.; Kunkel, S. R.; Przeworski, K. C.; Chass, G. A. *Angew. Chem., Int. Ed.* **2009**, *48*, 6836. (m) Saleh, N.; Blanchard, F.; Voituriez, A. *Adv. Synth. Catal.* **2017**, *359*, 2304. (n) Saleh, N.; Voituriez, A. *J. Org. Chem.* **2016**, *81*, 4371. (o) van Kalkeren, H. A.; Bruins, J. J.; Rutjes, F. P. J. T.; van Delft, F. L. *Adv. Synth. Catal.* **2012**, *354*, 1417. (p) Voituriez, A.; Saleh, N. *Tetrahedron Lett.* **2016**, *57*, 4443.

(3) van Kalkeren, H. A.; van Delft, F. L.; Rutjes, F. P. J. T. *ChemSusChem* **2013**, *6*, 1615.

(4) (a) Köhn, M.; Breinbauer, R. *Angew. Chem., Int. Ed.* **2004**, *43*, 3106. (b) Lin, F. L.; Hoyt, H. M.; van Halbeek, H.; Bergman, R. G.; Bertozzi, C. R. *J. Am. Chem. Soc.* **2005**, *127*, 2686. (c) Saxon, E.; Bertozzi, C. R. *Science* **2000**, *287*, 2007. (d) Schilling, C. I.; Jung, N.; Biskup, M.; Schepers, U.; Bräse, S. *Chem. Soc. Rev.* **2011**, *40*, 4840. (e) van Berkel, S. S.; van Eldijk, M. B.; van Hest, J. C. M. *Angew. Chem., Int. Ed.* **2011**, *50*, 8806. (f) Huang, D.; Yan, G. *Adv. Synth. Catal.* **2017**, *359*, 1600. (g) Liu, S.; Edgar, K. J. *Biomacromolecules* **2015**, *16*, 2556. (h) Mamat, C.; Gott, M.; Steinbach, J. *J. Labelled Compd. Radiopharm.* **2018**, *61*, 165.

(5) Andrews, K. G.; Denton, R. M. *Chem. Commun.* **2017**, *53*, 7982.

(6) Ruan, Z.; Lawrence, R. M.; Cooper, C. B. *Tetrahedron Lett.* **2006**, *47*, 7649.

DOI: 10.1021/acs.orglett.8b04035
Org. Lett. XXXX, XXX, XXX−XXX